A Letters Journal Exploring the Frontiers of Physics

November 2008

EPL, **84** (2008) 46004
doi: 10.1209/0295-5075/84/46004

www.epljournal.org

Contact mechanics with adhesion: Interfacial separation and contact area

C. Yang[1(a)], B. N. J. Persson[1], J. Israelachvili[2] and K. Rosenberg[2]

[1] *Institut für FestköperForschung, Forschungszentrum Jülich - D-52425 Jülich, Germany, EU*
[2] *Department of Chemical Engineering, University of California - Santa Barbara, CA 93106, USA*

received 26 August 2008; accepted in final form 21 October 2008
published online 21 November 2008

PACS 68.35.Np – Adhesion
PACS 81.40.Pq – Friction, lubrication, and wear
PACS 46.55.+d – Tribology and mechanical contacts

Abstract – We study the adhesive contact between elastic solids with randomly rough, self-affine fractal surfaces. We present molecular-dynamics (MD) simulation results for the interfacial stress distribution and the wall-wall separation. We compare the MD results for the relative contact area and the average interfacial separation, with the prediction of the contact mechanics theory of Persson. We find good agreement between theory and the simulation results. We apply the theory to the system studied by Benz *et al.* (*J. Phys. Chem. B*, **110** (2006) 11884) involving polymer in contact with polymer, but in this case the adhesion gives only a small modification of the interfacial separation as a function of the squeezing pressure.

With the rapid development of micro/nano electromechanical devices in the last decade, surface forces play a more and more important role in modern technology. This is due to the increase of the ratio between the number of atoms on the surface and that in the volume. When we bring two surfaces together, attractive (and repulsive) forces act between them, and a non-zero force is often required to separate two solid bodies placed in intimate contact [1,2], a phenomenon referred to as adhesion.

Adhesion manifests itself in many ways. Thus adhesion on one hand makes it possible for a Gecko to walk on the ceilings or run on a vertical wall [3,4]. On the other hand, adhesion can lead to the failure of micro or nano devices, *e.g.* micro-sized cantilever beams [5]. Thus, if it is too long or too thin, the free-energy minimum state corresponds to the cantilever beam partly bound to the substrate, which leads to the failure of the device. However, if the surface roughness is increased, the non-bonded cantilever state may be stabilized due to the decrease of cantilever-substrate binding energy.

In reality most surfaces are not atomically flat. Even if a surface appears flat at low magnification, when we study the surface at higher magnification we usually observe surface roughness on small length-scale. Similarly, when two solids with nominally smooth surfaces are brought into contact, generally they do not make contact everywhere, but at high enough magnification one usually observes many non-contact regions. The study of the interfacial separation is essential for describing, *e.g.*, sealing [6], capillary adhesion [7] or optical interference.

Contact mechanics between solid surfaces is the basis for understanding many tribology processes [8–11] such as friction, adhesion, wear and sealing. The two most important properties in contact mechanics are the area of real contact and the interfacial separation between the solid surfaces. For non-adhesive contact and small squeezing pressure, the average interfacial separation depends logarithmically on the squeezing pressure [12,13], and the (projected) contact area depends linearly on the squeezing pressure [14–16]. For adhesive contact, however, no numerical results have been presented in the literatures to test the contact mechanics theory with adhesion. In this letter, we study the relation between the average interfacial separation and the squeezing pressure when adhesion is included. We assume perfect (linear) elasticity and that the interfacial binding energy is independent of the separation speed, *i.e.*, we assume negligible hysteresis, as would be a good approximation for, *e.g.*, silicon rubber in contact with hard inert surfaces. We compare the result of MD simulations with a recently developed contact mechanics theory [13,14,17,18]. We find good agreement with the theory, which represents the first test of the

(a) E-mail: c.yang@fz-juelich.de

theory when the adhesive interaction is included in the analysis.

We review the contact mechanics theory of Persson briefly. It can be used to calculate the stress distribution at the interface, the area of real contact and the average interfacial separation between the solid walls [13,14]. In this theory, the interface is studied at different magnifications $\zeta = L/\lambda$ where L is the linear size of the system and λ the resolution. The wave vectors are defined as $q = 2\pi/\lambda$ and $q_L = 2\pi/L$ so that $\zeta = q/q_L$.

Consider an elastic block with a flat surface in adhesive contact with a hard substrate with a randomly rough surface. Let $\sigma(\mathbf{x}, \zeta)$ denote the (fluctuating) stress at the interface between the solids when the system is studied at the magnification ζ. The distribution of interfacial stress

$$P(\sigma, \zeta) = \langle \delta(\sigma - \sigma(\mathbf{x}, \zeta)) \rangle. \tag{1}$$

In this definition we do not include the $\delta(\sigma)$-contribution from the non-contact area.

For perfect (or complete) contact it is easy to show that $P(\sigma, \zeta)$ satisfies [14]

$$\frac{\partial P}{\partial \zeta} = f(\zeta) \frac{\partial^2 P}{\partial \sigma^2}, \tag{2}$$

where

$$f(\zeta) = \frac{\pi}{4} {E^*}^2 q_L q^3 C(q).$$

Here $E^* = E/(1-\nu^2)$ is the effective elastic modulus. The surface roughness power spectrum

$$C(q) = \frac{1}{(2\pi)^2} \int \mathrm{d}^2 x \ \langle h(\mathbf{x}) h(\mathbf{0}) \rangle e^{-i\mathbf{q}\cdot\mathbf{x}},$$

where $z = h(\mathbf{x})$ is the surface height at the point $\mathbf{x} = (x, y)$ and where $\langle .. \rangle$ stands for ensemble average. The basic idea is now to assume that (2) holds locally also for incomplete contact.

To solve (2), one needs boundary conditions. If we assume that, when studying the system at the lowest magnification $\zeta = 1$ (where no surface roughness can be observed, *i.e.*, the surfaces appear perfectly smooth), the stress at the interface is constant and equal to $p = F_{\mathrm{N}}/A_0$, where F_{N} is the load and A_0 the nominal contact area, then $P(\sigma, 1) = \delta(\sigma - p)$. In addition to this "initial condition" we need two boundary conditions along the σ-axis. Since there can be no infinitely large stress at the interface, we require $P(\sigma, \zeta) \to 0$ as $\sigma \to \infty$. For adhesive contact, which interests us here, tensile stress occurs at the interface close to the boundary lines of the contact regions. In this case we have the boundary condition $P(-\sigma_{\mathrm{a}}, \zeta) = 0$, where $\sigma_{\mathrm{a}} > 0$ is the largest tensile stress possible. The detachment stress $\sigma_{\mathrm{a}}(\zeta)$ depends on the magnification and can be related to the effective interfacial energy (per unit area) $\gamma_{\mathrm{eff}}(\zeta)$ using the theory of cracks [18]

$$\sigma_{\mathrm{a}}(\zeta) \approx \left(\frac{\gamma_{\mathrm{eff}}(\zeta) E q}{1-\nu^2} \right)^{1/2},$$

where

$$\gamma_{\mathrm{eff}}(\zeta) A^*(\zeta) = \Delta\gamma A^*(\zeta_1) - U_{\mathrm{el}}(\zeta),$$

where $A^*(\zeta)$ denotes the total contact area at the magnification ζ, which is larger than the projected contact area $A(\zeta)$. $U_{\mathrm{el}}(\zeta)$ is the elastic energy stored at the interface due to the elastic deformation of the solids on a length scale shorter than $\lambda = L/\zeta$, necessary in order to bring the solids into adhesive contact (see below).

From (2) it follows that the area of apparent contact (projected on the xy-plane) at the magnification ζ, $A(\zeta)$, normalized by the nominal contact area A_0, can be obtained from

$$\frac{A(\zeta)}{A_0} = \int_{-\sigma_{\mathrm{a}}(\zeta)}^{\infty} \mathrm{d}\sigma \, P(\sigma, \zeta). \tag{3}$$

We denote $A(\zeta)/A_0 = P_p(q)$, where the index p indicates that $A(\zeta)/A_0$ depends on the applied squeezing pressure p. The area of (apparent) contact at the highest magnification $\zeta = \zeta_1$ gives the real contact area. For the elastic energy U_{el} we use [19]

$$U_{\mathrm{el}} \approx A_0 E^* \frac{\pi}{2} \int_{q_L}^{q_1} \mathrm{d}q \, q^2 W(q, p) C(q), \tag{4}$$

where q_L and q_1 are the smallest and the largest surface roughness wave vectors, and [19]

$$W(q, p) = P_p(q) \left[\beta + (1-\beta) P_p^2(q) \right],$$

where $\beta = 0.4$. The equations given above are solved as described in ref. [17].

Let us now consider the (average) interfacial separation $\bar{u}$ as a function of the squeezing pressure $p = F_{\mathrm{N}}/A_0$. Note that as p increases, $\bar{u}$ decreases and we can consider $p = p(\bar{u})$ as a function of $\bar{u}$. Energy conservation gives [18]

$$\int_{\bar{u}}^{\infty} \mathrm{d}u \, p(u) A_0 = U, \tag{5}$$

where $U = U_{\mathrm{el}} + U_{\mathrm{ad}}$ is the sum of the elastic energy U_{el} stored at the interface and given by (4), and the adhesional energy $U_{\mathrm{ad}} = -\Delta\gamma A^*(\zeta_1)$. From (5) we get

$$p(\bar{u}) = -\frac{1}{A_0} \frac{\mathrm{d}U(\bar{u})}{\mathrm{d}\bar{u}}.$$

We can also consider U as a function of p and write

$$p(\bar{u}) = -\frac{1}{A_0} \frac{\mathrm{d}U}{\mathrm{d}p} \frac{\mathrm{d}p}{\mathrm{d}\bar{u}},$$

or

$$\mathrm{d}\bar{u} = -\frac{1}{A_0 p} \frac{\mathrm{d}U}{\mathrm{d}p} \mathrm{d}p.$$

Integrating from $u=0$ (corresponding to $p=\infty$) to u (corresponding to the pressure p) gives

$$\bar{u} = \frac{1}{A_0}\int_p^\infty \mathrm{d}p\ \frac{1}{p}\frac{\mathrm{d}U}{\mathrm{d}p}, \tag{6}$$

which is very convenient for numerical calculations.

Let us provide some details about the numerical simulations. The molecular-dynamics system has lateral dimension $L_x = N_x a$ and $L_y = N_y a$, where a is the lattice spacing of the block. In order to accurately study contact mechanics between elastic solids, it is necessary to consider that the thickness of the block is (at least) of the same order of the lateral size of the longest-wavelength roughness on the substrate. We have developed a multiscale MD approach to study contact mechanics [20]. Periodic boundary condition has been used in the xy-plane. For the block $N_x = N_y = 400$, while the lattice space of the substrate $b \approx a/\phi$, where $\phi = (1+\sqrt{5})/2$ is the golden mean, in order to avoid the formation of commensurate structures at the interface. The mass of the block atoms is 197 a.m.u. and $a = 2.6\,\text{Å}$. The elastic modulus and Poisson ratio of the block are $E = 77.2\,\text{GPa}$ and $\nu = 0.42$. For self-affine fractal surfaces, the power spectrum has power law behavior $C(q) \sim q^{-2(H+1)}$, where the Hurst exponent H is related to the fractal dimension D_f of the surface via $H = 3 - D_f$. For real surfaces this relation holds only for a finite wave vector region $q_0 < q < q_1$. Note that in many cases, there is a roll-off wave vector q_0 below which $C(q)$ is approximately constant. Here we use $q_L = 2\pi/L, q_0 = 3q_L, q_1 = 12q_L$. q_0 is named as roll-off wave vector. The physical meaning is that by choosing $q_0 = 3q_L$ one can obtain a self-average equivalent to an average over 9 independent samples. In MD simulations, the substrate is rigid and fractal with fractal dimension $D_f = 2.2$ and root-mean-square roughness $h_{\text{rms}} = 10\,\text{Å}$. The calculations are carried out under the temperature 0 K. The contact in the present study has been generated by increasing pressure stepwisely from non-contact to large contact condition [21]. It can be also done in the opposite way by retracting the block from the substrate, that is the contact will be generated from large contact to non-contact. These two situations will in general give different results, especially when the material is non-elastic, as is what we called "contact hysteresis". It will be our further study and will be reported elsewhere.

The atoms at the interface between block and substrate interact with the potential

$$V(r) = 4\epsilon\left[\left(\frac{r_0}{r}\right)^{12} - \left(\frac{r_0}{r}\right)^{6}\right],$$

where r is the distance between the pair of atoms. The parameter ϵ is the binding energy between two atoms at separation $r = 2^{1/6} r_0$. In the calculations presented below we have used the $r_0 = 3.28\,\text{Å}$ and $\epsilon = \epsilon_0$, $4\epsilon_0$ and $8\epsilon_0$, where $\epsilon_0 = 18.6\,\text{meV}$. By comparing the total energy for the surfaces separated with the case where the surfaces are in contact at equilibrium (at zero external load) we obtain $\Delta\gamma = 0.69\,\text{J/m}^2$ for the case $\epsilon = \epsilon_0$, and 4 and 8 times higher interfacial binding energy for the other two cases, respectively.

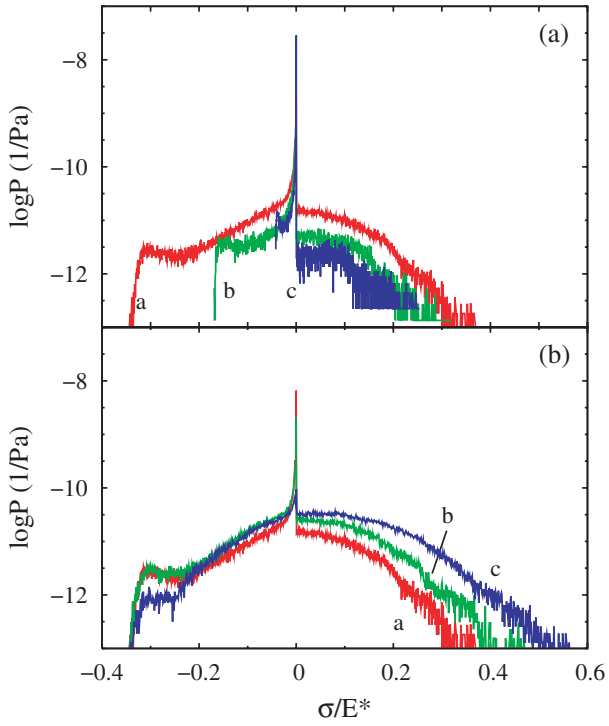

Fig. 1: The logarithm (with 10 as basis) of the probability distribution of normal stress σ (where σ is in units of E^*) for (a) three different adhesion parameters $\epsilon = 8\epsilon_0$, $4\epsilon_0$ and ϵ_0, referred to as a, b and c, respectively, and (b) with $8\epsilon_0$ for three different pressures $p/E^* = -0.00532$, 0.00832, 0.06265 denoted by a,b, and c, respectively.

Now, let us discuss how to define contact on the atomic scale when adhesion is included. In the absence of adhesion we have found that the interfacial stress distribution gives the most accurate way of deducing the area of real contact [20]. When adhesion is included we use a cut-off length d_c to define contact. It is clear from the force-distance curve that the only distinctive point is the maximum tensile stress [22]. Thus the solids are regarded as in contact when the stress increases with separation, and separated when the stress decreases with separation. In our case, the critical wall-wall distance is $d_c = 3.68\,\text{Å}$. When the interfacial separation $d < d_c$, it is defined as contact. Otherwise it is non-contact. More discussions about d_c can be found in ref. [23].

The probability distribution of (perpendicular) stress σ at the interface is shown in fig. 1 for (a) the adhesion parameter $\epsilon = \epsilon_0$, $4\epsilon_0$ and $8\epsilon_0$, and (b) for $\epsilon = 8\epsilon_0$ for three different values of the applied stress p ($p/E^* = -0.00532$, 0.00832 and 0.06265). Note that when ϵ increases, the maximum σ_c of the tensile stress increases roughly proportional to ϵ. In fact, we expect $\sigma_c \propto \epsilon/a$, where a is of order a bond length. At the same time the maximum repulsive pressure increases but weaker than linear. The increase in

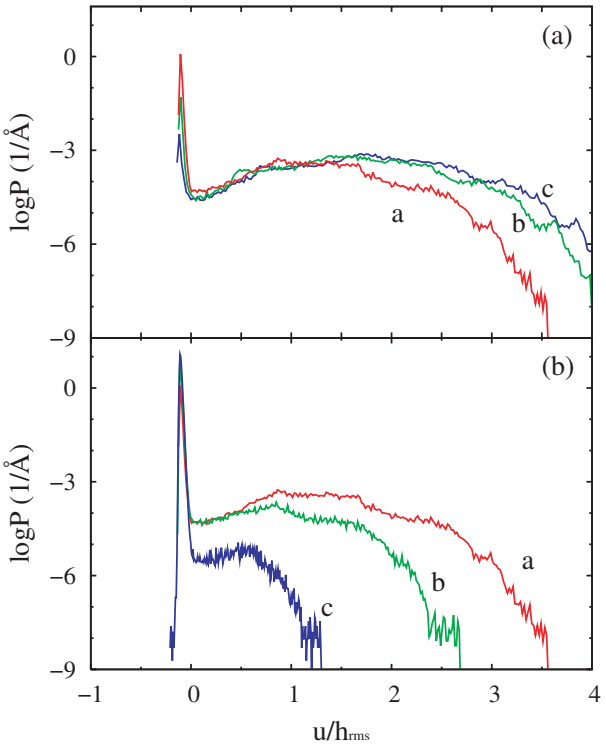

Fig. 2: The logarithm (with 10 as basis) of the probability distribution of interfacial separations u (where u is in units of the root-mean-square roughness amplitude $h_{\rm rms}$) for (a) three different adhesion parameters $\epsilon = 8\epsilon_0$, $4\epsilon_0$ and ϵ_0, referred to as a, b and c, respectively, and (b) with $8\epsilon_0$ for three different pressures $p/E^* = -0.00532$, 0.00832, 0.06265 denoted by a, b, and c, respectively.

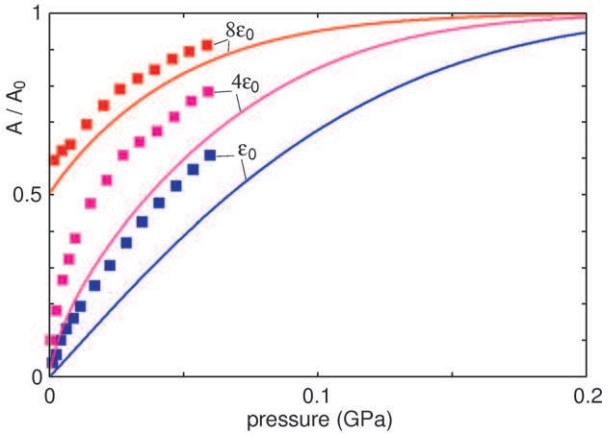

Fig. 3: Molecular-dynamics (square symbols) and theoretical (solid lines) results for the relative contact area A/A_0 as a function of the squeezing pressure (in GPa) In the calculation (solid lines) we have used $\Delta\gamma = 0.7$, 2.8 and $5.6\,{\rm J/m^2}$ for the curves indicated by ϵ_0, $4\epsilon_0$ and $8\epsilon_0$, respectively. The theoretical results are obtained from eq. (3).

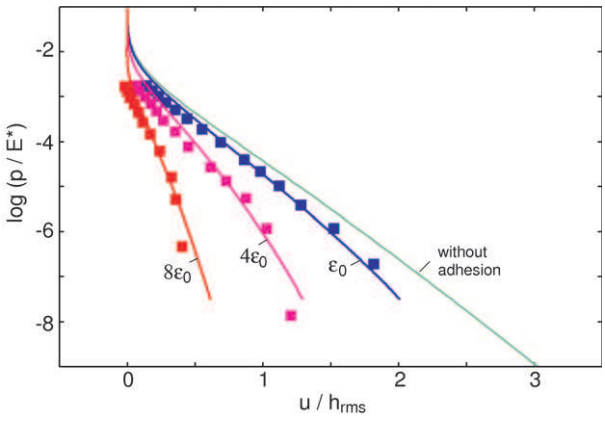

Fig. 4: Molecular-dynamics (square symbols) and theoretical (solid lines) results for the (natural) logarithm of the squeezing pressure p (in units of E^*) as a function of the average interfacial separation $\bar{u}$ in units of the root-mean-square roughness amplitude $h_{\rm rms}$. The theoretical results are obtained from eq. (6).

repulsive stress is, of course, due to the additionally adhesional load which acts on the block.

When the applied load or pressure increases, the maximal tensile stress is unchanged, see fig. 1(b). This is the expected result since the maximum tensile stress is associated with breaking the atomic bonds at the edges of the contact regions (which can be considered as crack tips), and this stress is of course independent of the load. However, the maximum repulsive stress increases with load, but the effect is quite small considering the large change in the load.

The probability distribution of interfacial separations is shown in fig. 2. In fig. 2(a) we vary the adhesion parameter ϵ and in (b) the applied stress p as in fig. 1. When the adhesion increases, the surfaces are pulled closer to each other and the distribution of separations becomes narrower. Similarly, when the applied pressure increases, the separation between the walls decreases.

The MD simulations (square symbols) are compared with the theory (solid lines) for the relative contact area A/A_0 as a function of the squeezing pressure p (see fig. 3). In fig. 4 we show the (natural) logarithm of the squeezing pressure p (in units of E^*) as a function of the average interfacial separation $\bar{u}$ in units of the root-mean-square roughness amplitude $h_{\rm rms}$. The theoretical results (solid lines) agree very well with the molecular-dynamics calculations (square symbols).

Benz *et al.* [12] have studied the contact mechanics for polymer surfaces. They studied the interfacial separation as a function of the squeezing pressure, and found an absolute (average) slope bigger than the one obtained from finite element calculations [24] for non-adhesive contact between the interfacial separation and the log-scale pressure. For adhesive contact, both theory and MD simulations predict a bigger absolute (average) slope than the one for non-adhesive contact (see fig. 4). However for the system studied by Benz *et al.* [12] we find that the adhesional interaction gives only a very small ($\approx 20\%$) increase in the absolute (average) slope, which cannot

explain the experimental results by Benz *et al.* [12]. In ref. [25] we present a critical analysis of this point. For non-adhesive contact, a recent experimental study (using silicon rubber) by Lorenz and Persson [26] finds nearly perfect agreement between experiment and theory for the interfacial separation as a function of load.

To summarize, we have presented a molecular-dynamics (MD) study of the adhesive contact between elastic solids with randomly rough surfaces. We have calculated the contact area and the interfacial separation between the elastic solids, and compared the results with the predictions of a recently developed contact mechanics model, which is based on continuum mechanics. Considering the uncertainty in how to define the contact area and the interfacial separation at the atomistic level, and the small size of our MD system, the agreement between the theory and the MD results is very good.

* * *

We thank U. Tartaglino for many useful discussions.

REFERENCES

[1] Johnson K. L., Kendall K. and Roberts A. D., *Proc. R. Soc. London, Ser. A*, **324** (1971) 301.

[2] Fuller K. N. G. and Tabor D., *Proc. R. Soc. London, Ser. A*, **345** (1975) 327.

[3] Gao H. and Yao H., *Proc. Natl. Acad. Sci. U.S.A.*, **101** (2004) 7851.

[4] Autumn K. and Gravish N., *Philos. Trans. R. Soc. A*, **366** (2008) 1575.

[5] Zhao Y. P., Wang L. S. and Yu T. X., *J. Adv. Sci. Technol.*, **17** (2003) 519.

[6] Persson B. N. J. and Yang C., *J. Phys.: Condens. Matter*, **20** (2008) 315011.

[7] Persson B. N. J., *J. Phys.: Condens. Matter*, **20** (2008) 315007.

[8] Bowden F. P. and Tabor D., *Friction and Lubrication of Solids* (Wiley, New York) 1956.

[9] Johnson K. L., *Contact Mechanics* (Cambridge University Press, Cambridge) 1966.

[10] Persson B. N. J., *Sliding Friction: Physical Principles and Applications,* 2nd edition (Springer, Heidelberg) 2000.

[11] Israelachvili J. N., *Intermolecular and Surface Forces* (Academic, London) 1995.

[12] Benz M., Rosenberg K. J., Kramer E. J. and Israelachvili J. N., *J. Phys. Chem. B*, **110** (2006) 11884.

[13] Persson B. N. J., *Phys. Rev. Lett.*, **99** (2007) 125502.

[14] Persson B. N. J., *J. Chem. Phys.*, **115** (2001) 3840.

[15] Greenwood J. A. and Williamson J. B. P., *Proc. R. Soc. London, Ser. A*, **295** (1966) 300.

[16] Müser M. H., *Phys. Rev. Lett.*, **100** (2008) 055504.

[17] Persson B. N. J., *Eur. Phys. J. E*, **8** (2002) 385.

[18] Persson B. N. J., *Surf. Sci. Rep.*, **61** (2006) 201.

[19] Yang C. and Persson B. N. J., *J. Phys.: Condens. Matter*, **20** (2008) 215214.

[20] Yang C., Tartaglino U. and Persson B. N. J., *Eur. Phys. J. E*, **19** (2006) 47.

[21] Yang C. and Persson B. N. J., *Phys. Rev. Lett.*, **100** (2008) 024303.

[22] Greenwood J. A., *Proc. R. Soc. London, Ser. A*, **453** (1997) 1277.

[23] Yang C., *Role of Surface Roughness in Tribology: From Atomic to Macroscopic Scale* (Forschungszentrum Jülich) 2008.

[24] Pei L., Hyun S., Molinari J. F. and Robbins M. O., *J. Mech. Phys. Solids*, **53** (2005) 2385.

[25] See document arXiv:0810.2976 for a critical discussion of the experimental data presented in ref. [12]. For more information on arXiv, see `http://arxiv.org/abs/0810.2976`.

[26] Lorenz B. and Persson B. N. J., to be published in *J. Phys.: Condens. Matter*.